2376 *Inorg. Chem.* **1990**, *29*, 2376-2381

Contribution from the Department of Chemistry, University of Notre Dame, Notre Dame, Indiana 46556,
Center for Catalytic Science and Technology, Department of Chemical Engineering, University of Delaware, Newark, Delaware 19716,
and Dipartimento di Chimica "G. Ciamician", Universita di Bologna, Via F. Selmi 2, I-40126, Bologna, Italy

Interaction of $Ru_3(CO)_{12}$ with Silanols and Silanolate Groups. X-ray Crystal Structure Analysis of (μ-H)$Ru_3(CO)_{10}$(μ-$OSiEt_3$), a Molecular Analogue of a Silica-Supported Metal Cluster

Jose Puga,*,†,[1a,b] Thomas P. Fehlner,[1a] Bruce C. Gates,[1b] Dario Braga,*,[1c] and Fabrizia Grepioni[1c]

Received June 30, 1989

Interaction of $Ru_3(CO)_{12-x}L_x$ (L = CO, NCMe; x = 1, 2) with R_3SiOH (R = Et, Ph), Ph_3SiONa, AlH_3, and $Et_3N\cdot AlH_3$ has been found to yield exclusively reduction products (i.e., $H_2Ru_4(CO)_{13}$, $H_2Ru_6(CO)_{18}$, $[Ru_3(CO)_{11}]^{2-}$, $[Ru_4(CO)_{13}]^{2-}$, $[Ru_6(CO)_{18}]^{2-}$, and $[HRu_3(CO)_{11}]^-$). However, reaction of the triethylsilanol derivative with $Ru_3(CO)_{12}$, in the presence of catalytic amounts of $Cp_2Fe_2(CO)_4$, occurred via oxidative addition to a Ru–Ru bond to afford (μ-H)$Ru_3(CO)_{10}$(μ-$OSiEt_3$) (**1**), 7% yield. Structural characterization of **1** was carried out by single-crystal X-ray diffraction. Crystal data: space group $C2/c$, a = 29.213 (7) Å, b = 11.358 (2) Å, c = 15.409 (2) Å, β = 107.42 (1)°, V = 4878.23 Å^3, Z = 8. Compound **1** has a triangular metal framework with a μ-$OSiEt_3$ group spanning one edge. The hydride ligand is found bridging the same Ru–Ru bond [Ru–H = 1.74 (2) Å].

Introduction

Incorporation of main-group elements within a metal cluster framework has led to improved understanding of a variety of chemical processes. For example, investigation of the synthesis and reactivity of carbidometal clusters has given mechanistic insight into the chemisorption and hydrogenation of carbon monoxide on surfaces.[2-6] Likewise, boron-containing metal clusters, e.g. $HFe_4(CO)_{12}BH_2$,[7] have been used as precursors for the preparation of metallic glasses,[8] and the first example of an encapsulated metal boride cluster, $[Fe_4Rh_2(CO)_{16}B]^-$, has been reported.[9] The synthesis and structural characterization of $HOs_3(CO)_{10}$(μ-$OSiEt_3$) has shed light on the nature of the chemisorption of metal clusters on metal oxide surfaces,[10] providing a bridge between solution and surface organometallic chemistry. The latter compound and its surface-bound analogue have been found to be catalysts for the hydrogenation of alkenes.[11,12] The reactivity of metal carbonyl clusters with group IIIB and group IVB compounds is complicated, often dominated by the reductive nature of these reactants. Nonetheless this approach has yielded a rich variety of derivatives containing main-group elements interacting directly with metals. Good examples are the metal-rich metallaboranes in which main-group element fragments are stabilized by coordination to transition metals.[13,14]

This contribution is a report of the interaction of $Ru_3(CO)_{12-x}L_x$ (L = CO, NCMe; x = 1, 2) with IIIB and IVB group compounds, specifically Al and Si complexes. Our interest in the interaction of silanols and silanolates with carbonyl compounds derives from the value of the products as molecular models of surface species, and the reactivities are analyzed in this context. The results include the structure analysis of (μ-H)$Ru_3(CO)_{10}$(μ-$OSiEt_3$), an analogue of a silica-supported triruthenium cluster.

Experimental Section

Tetrahydrofuran (THF), diethyl ether, and hexane were used after being freshly distilled from sodium–benzophenone under nitrogen. Dichloromethane and acetonitrile were distilled from P_2O_5. Cyclohexane (Aldrich) was degassed; triphenylsilanol was used without further purification. All procedures were performed under nitrogen. $LiAlH_4$, $AlCl_3$, $LiEt_3BH$, and $Ru_3(CO)_{12}$ (Strem) were used as received. AlH_3, $Et_3N\cdot AlH_3$, $Ru_3(CO)_{12-x}L_x$ (L = NCMe; x = 1, 2), and Ph_3SiONa were prepared according to literature procedures.[15-17] Infrared spectra were recorded on Nicolet 7199 FT, IBM IR-32 FT, and Perkin-Elmer 1420 spectrophotometers. ^1H NMR spectra were recorded on a Nicolet 300-MHz spectrometer. Mass spectra were obtained with an AEI-MS 9 spectrometer.

Reaction of $Ru_3(CO)_{10}(NCMe)_2$ with R_3SiOH (R = Et, Ph). Similar procedures were followed for the two different silanols, with essentially the same results. In a typical experiment, Et_3SiOH (64 mg, 0.48 mmol) was added to an acetonitrile solution of $Ru_3(CO)_{10}(NCMe)_2$ (150 mg, 0.23 mmol). The mixture was stirred for ca. 24 h at room temperature. Workup of the solution gave $Ru_3(CO)_{12}$ (106 mg; yield 80%) (hexane: 2061 vs, 2031 s, 2019 m cm^{-1}).

Reaction of $Ru_3(CO)_{10}(NCMe)_2$ with Et_3SiOH in the Absence of Solvent. $Ru_3(CO)_{10}(NCMe)_2$ (80 mg, 0.11 mmol) was allowed to react with Et_3SiOH (10 mL) at 55 °C for ca. 1 h. Workup of the solution yielded $Ru_3(CO)_{12}$ (42 mg; yield 60%), $H_2Ru_6(CO)_{18}$ (13 mg; yield 10%) (CH_2Cl_2: 2060 s, 2054 s sh, 2027 w cm^{-1}), and $H_2Ru_4(CO)_{13}$ (12 mg; yield 13%) (hexane: 2077 s, 2066 vs, 2055 vs, 2033 m sh, 2024 m, 2012 w cm^{-1}). When the reaction was carried out at 70 °C, considerable decomposition occurred, and $Ru_3(CO)_{12}$ was obtained as the only identified species.

Reaction of $Ru_3(CO)_{10}L_2$ (L = CO, NCMe) with Ph_3SiONa. A. A solution of Ph_3SiONa (54 mg, 0.18 mmol) in THF was added to solid $Ru_3(CO)_{10}(NCMe)_2$ (40 mg, 0.060 mmol). The IR spectrum of the solution revealed bands at 2014 m, 1984 m sh, 1986 s sh, 1956 s, and 1929 w cm^{-1}, assigned to $[Ru_3(CO)_{11}]^{2-}$.

B. To a THF solution of $Ru_3(CO)_{12}$ (100 mg, 0.16 mmol) was slowly added Ph_3SiONa (48 mg, 0.16 mmol), dissolved in THF. Formation of $[Ru_6(CO)_{18}]^{2-}$ (2003 m sh, 1988 s, 1937 m cm^{-1}) and $[Ru_4(CO)_{13}]^{2-}$ (1943 m cm^{-1}) was observed. Protonation of the anionic species with H_2SO_4 in CH_2Cl_2 gave $H_2Ru_6(CO)_{18}$ (53 mg; yield 30%) [identified by IR spectroscopy (CH_2Cl_2: 2060 s, 2054 s sh, 2027 w, 2007 w cm^{-1}) and by single-crystal X-ray diffraction determination of the unit cell parameters], unreacted $Ru_3(CO)_{12}$ (22 mg), and $H_2Ru_4(CO)_{13}$ (25 mg; yield 20%) [identified by IR spectroscopy (hexane: 2077 s, 2066 vs, 2055 vs, 2033 m sh, 2024 m, 2012 w cm^{-1}) and by determination of the unit cell parameters using single-crystal X-ray diffractometry].

C. $Ru_3(CO)_{12}$ (100 mg, 0.16 mmol) was slowly added to a THF

---

† Current address: The Dow Chemical Co., Central Research, Catalysis Laboratory, 1776 Building, Midland, MI 48674.

(1) (a) University of Notre Dame. (b) University of Delaware. (c) University of Bologna.

(2) Muetterties, E. L.; Rhodin, T. N.; Band, E.; Brucker, C. P. *Chem. Rev.* **1979**, *79*, 91–137.

(3) Muetterties, E. L.; Stein, J. *Chem. Rev.* **1979**, *79*, 479–490.

(4) Bradley, J. S. *Adv. Organomet. Chem.* **1983**, *22*, 1–58.

(5) Shriver, D. F.; Sailor, M. J. *Acc. Chem. Res.* **1988**, *21*, 374–379.

(6) Steinmetz, G. R.; Morrison, E. D.; Geoffroy, G. L. *J. Am. Chem. Soc.* **1984**, *106*, 2559–2564.

(7) Housecroft, C. E.; Fehlner, T. P.; Buhl, M. L.; Long, G. L. *J. Am. Chem. Soc.* **1987**, *109*, 3323–3329.

(8) Amini, M. M.; Zeller, M. V.; Stickle, W. F.; Pruigle, O. A.; Long, G. J.; Felhner, T. P. *Mater. Res. Soc. Symp. Proc.* **1989**, *131*, 413–418.

(9) Khattar, R.; Puga, J.; Fehlner, T. P.; Rheingold, A. L. *J. Am. Chem. Soc.* **1989**, *111*, 1877–1879.

(10) D'Ornelas, L.; Choplin, A.; Basset, J. M.; Hsu, L. Y.; Shore, S. G. *Nouv. J. Chim.* **1985**, *9*, 155–157.

(11) Besson, B.; Choplin, A.; D'Ornelas, L.; Basset, J. M. *J. Chem. Soc., Chem. Commun.* **1982**, 843–845.

(12) Choplin, A.; Besson, B.; D'Ornelas, L.; Sanchez-Delgado, R.; Basset, J. M. *J. Am. Chem. Soc.* **1988**, *110*, 2783–2787.

(13) Fehlner, T. P. *New J. Chem.* **1988**, *12*, 307–316.

(14) Housecroft, C. E. *Polyhedron* **1987**, *6*, 1955–1958.

(15) Foulds, G. A.; Johnson, B. F. G.; Lewis, J. *J. Organomet. Chem.* **1985**, *296*, 147–153.

(16) Eaborn, C. *Organosilicon Compounds*; Butterworths: London, 1960; p 272.

(17) Ruff, J. K.; Hawthorne, M. F. *J. Am. Chem. Soc.* **1960**, *82*, 2141–2144.

(18) Walker, N.; Stuart, D. *Acta Crystallogr.* **1983**, *A39*, 158–166.

0020-1669/90/1329-2376$02.50/0

Table I. Selected Bond Distances (Å) and Angles (deg) for $(\mu\text{-H})Ru_3(CO)_{10}(\mu\text{-OSiEt}_3)$

Ru(1)–Ru(2)	2.796 (1)	C(6)–O(6)	1.149 (7)
Ru(1)–Ru(3)	2.753 (1)	C(7)–O(7)	1.123 (7)
Ru(2)–Ru(3)	2.792 (1)	C(8)–O(8)	1.122 (7)
Ru(1)–C(1)	1.950 (6)	C(9)–O(9)	1.125 (7)
Ru(1)–C(2)	1.906 (6)	Ru(1)–O(11)	2.106 (3)
Ru(1)–C(3)	1.870 (6)	Ru(3)–O(11)	2.107 (3)
Ru(3)–C(4)	1.945 (5)	Si–O(11)	1.648 (3)
Ru(3)–C(5)	1.859 (6)	Si–C(11)	1.871 (8)
Ru(3)–C(6)	1.893 (6)	Si–C(13)	1.882 (7)
Ru(2)–C(7)	1.933 (6)	Si–C(15)	1.870 (7)
Ru(2)–C(8)	1.927 (6)	C(11)–C(12)	1.49 (1)
Ru(2)–C(9)	1.929 (6)	C(13)–C(14)	1.48 (1)
C(1)–O(1)	1.133 (7)	C(15)–C(16)	1.52 (1)
C(2)–O(2)	1.120 (7)	C(10)–O(10)	1.138 (7)
C(3)–O(3)	1.138 (6)	Ru(1)–H(16)	1.75 (1)
C(4)–O(4)	1.123 (6)	Ru(3)–H(16)	1.74 (1)
C(5)–O(5)	1.140 (7)	Ru(2)–C(10)	1.928 (6)

Ru(1)O(11)–Si	134.4 (2)	Ru(1)–C(3)–O(3)	177.6 (5)
Ru(3)–O(11)–Si	131.9 (2)	Ru(3)–C(4)–O(4)	171.3 (5)
O(11)–Si–C(11)	106.6 (3)	Ru(3)–C(5)–O(5)	177.7 (5)
O(11)–Si–C(13)	111.2 (2)	Ru(3)–C(6)–O(6)	179.5 (5)
O(11)–Si–C(15)	108.8 (3)	Ru(2)–C(7)–O(7)	177.4 (5)
Ru(1)–H(16)–Ru(3)	104.2 (6)	Ru(2)–C(8)–O(8)	178.3 (7)
Ru(1)–C(1)–O(1)	170.8 (6)	Ru(2)–C(9)–O(9)	177.9 (6)
Ru(1)–C(2)–O(2)	178.4 (6)		

solution of Ph_3SiONa (48 mg, 0.16 mmol). The reaction was monitored by IR spectroscopy. Formation of $[Ru_3(CO)_{11}]^{2-}$ (2014 m, 1962 s sh, 1949 s, 1928 m cm^{-1}) was observed. Upon addition of $Ru_3(CO)_{12}$, a band at 1987 cm^{-1}, assigned to $[Ru_6(CO)_{18}]^{2-}$, was detected. The final stages of the reaction clearly showed the formation of $[Ru_6(CO)_{18}]^{2-}$ (2003 m sh, 1988 s, 1937 m cm^{-1}) and $[Ru_4(CO)_{13}]^{2-}$ (1953 m cm^{-1}) at the expense of the trinuclear dianion. Protonation of these anionic species in THF with H_2SO_4 gave $H_2Ru_4(CO)_{13}$ (21 mg; yield 23%, based on $Ru_3(CO)_{12}$), and $[HRu_6(CO)_{18}]^-$ (10.4 mg; yield 44%, based on $Ru_3(CO)_{12}$) (THF: 2022 s, 1960 w br cm^{-1}).

Reaction of $Ru_3(CO)_{11}L$ (L = CO, NCMe) with AlH_3 and $Et_3N{\cdot}AlH_3$. A 0.1 M solution of AlH_3 in diethyl ether was slowly added to $Ru_3(CO)_{12}$ (100 g, 0.16 mmol), dissolved in THF, at −20 °C. Formation of $[HRu_3(CO)_{11}]^-$ (2065 m, 2014 vs, 1987 vs, 1951 s cm^{-1}) was observed; further addition of AlH_3 was followed by precipitation of a brown solid, rather insoluble in common organic solvents. The IR spectrum of the species in solution indicated the presence of $[Ru_3(CO)_{11}]^{2-}$. Protonation of the anionic compound with HBF_4 gave $H_2Ru_4(CO)_{13}$ (37 mg; yield 40%, based on $Ru_3(CO)_{12}$) and $H_4Ru_4(CO)_{12}$ (18 mg; yield 20%, based on $Ru_3(CO)_{12}$) (hexane: 1980 s, 2064 vs, 2022 s cm^{-1}). The reaction was also performed at −50 °C with similar results. Essentially the same distribution of products was obtained when superhydride ($LiEt_3BH$) was brought into contact with $Ru_3(CO)_{12}$ followed by addition of AlH_3.

Reaction of $Ru_3(CO)_{12}$ with $Et_3N{\cdot}AlH_3$ produced, after stirring at room temperature for ca. 4 days, an unidentified brown solid, which was rather insoluble in common organic solvents. Interaction with $Ru_3(CO)_{11}(NCMe)$, on the other hand, resulted in formation of $[Ru_3(CO)_{11}]^{2-}$, as identified by IR spectroscopy.

Reaction of $Ru_3(CO)_{12}$ with Et_3SiOH in the Presence of $[FeCp(CO)_2]_2$. $Ru_3(CO)_{12}$ (200 mg, 0.31 mmol) and $[FeCp(CO)_2]_2$ (10.6 mg, 0.03 mmol) were heated to 80 °C, and Et_3SiOH (0.7 mL) was added. The mixture was refluxed for ca. 3 h followed by evaporation of the solvent under vacuum. The residue was extracted with pentane (35 mL). The extract was concentrated and purified by thin-layer chromatography using hexane as eluent. A top orange band was extracted with dichloromethane and identified as $(\mu\text{-H})Ru_3(CO)_{10}(\mu\text{-OSiEt}_3)$ (15 mg; yield 7%) by IR (hexane: 2105 w, 2068 vs, 2057 s, 2022 vs, 2008 s, 2000 m sh, 1995 m cm^{-1}) and ^1H NMR spectroscopy ($CDCl_3$: 0.97 t, 0.59 q, −12.08 s ppm; integration ratio 9:6:1) and mass spectrometry (*m/e* 715, ^{101}Ru, ^{28}Si, fragmentation pattern corresponding to sequential loss of 10 CO's). The second top band was identified as unreacted $Ru_3(CO)_{12}$ (102 mg), and the third band, as $H_2Ru_4(CO)_{13}$ (24 mg; yield 10%).

Crystallographic Analysis. Crystals suitable for X-ray diffraction were obtained by slow evaporation of a dichloromethane–hexane solution. Diffraction intensities were collected at room temperature on an Enraf-Nonius CAD-4 diffractometer with Mo Kα radiation (λ = 0.71069 Å). Crystal data and details of measurements are summarized in Table II. Intensities were corrected for Lorentz and polarization factors. The structure was solved by direct methods, which allowed location of the Ru atoms to be established. All other atoms were then located from subsequent difference-Fourier synthesis. Absorption correction was applied by the Walker and Stuart method.[19] Once a complete structural model had been obtained and all atoms refined isotropically (correction range 0.89–1.10), H atoms of the C_2H_5 groups were added in calculated positions (C–H = 1.08 Å) and refined "riding" on their corresponding C atoms. All but the H atoms were allowed to vibrate anisotropically, and single isotropic thermal parameters were assigned to the $H(CH_2)$ and $H(CH_3)$ atoms and refined independently [0.12 (1) and 0.19 (1) $Å^2$, respectively]. The final Fourier maps showed a peak of ca. 1 e $Å^{-3}$ in a bridging position between the Ru(1) and Ru(3) atoms, which was attributed to the H (hydride) atom. This position was refined by constraining the Ru–H bonds to the distances obtained from the Fourier synthesis, and an isotropic thermal parameter [0.076 (2) $Å^2$] was also refined. The final *R* value was 0.039 (R_w = 0.039). Residual peaks of ca. 0.5 e $Å^{-3}$ were located in the proximity of the Ru atoms. For all calculations, the SHELX76[19] package of crystallographic programs was used. Atomic scattering factors were taken from ref 20. The final

Table II. Crystal Data for $(\mu\text{-H})Ru_3(CO)_{10}(\mu\text{-OSiEt}_3)$

formula	$C_{16}H_{16}O_{11}Ru_3Si$
M_r	715.58
cryst size, mm	0.10 × 0.12 × 0.14
syst	monoclinic
space group	*C*2/*c*
a, Å	29.213 (7)
b, Å	11.358 (2)
c, Å	15.409 (2)
β, deg	107.42 (1)
V, $Å^3$	4878.23
Z	8
F(000)	2768
D_c, 9 cm^{-3}	1.95
λ(Mo Kα), Å	0.71069
μ(Mo Kα), cm^{-1}	17.49
R	0.0390
R_w[a]	0.039

[a] $R_w = [(F_o - F_c)w^{1/2}]/(F_ow^{1/2})$, where $w = k/[\delta(F) + |g|F^2]$.

Table III. Fractional Atomic Coordinates for $(\mu\text{-H})Ru_3(CO)_{10}(\mu\text{-OSiEt}_3)$

atom	*x*	*y*	*z*
Ru(1)	0.08091 (1)	0.18891 (3)	0.62329 (2)
Ru(2)	0.15049 (1)	0.05294 (3)	0.57882 (3)
Ru(3)	0.10705 (1)	0.24319 (3)	0.47057 (2)
C(1)	0.0277 (2)	0.2831 (5)	0.6370 (4)
O(1)	−0.0058 (2)	0.3239 (5)	0.6471 (4)
C(2)	0.1139 (2)	0.1707 (5)	0.7495 (4)
O(2)	0.1324 (2)	0.1587 (5)	0.8239 (3)
C(3)	0.0457 (2)	0.0509 (5)	0.6215 (3)
O(3)	0.0232 (2)	−0.0316 (4)	0.6177 (3)
C(4)	0.0691 (2)	0.3687 (5)	0.3973 (3)
O(4)	0.0470 (2)	0.4325 (4)	0.3460 (3)
C(5)	0.0887 (2)	0.1403 (5)	0.3724 (4)
O(5)	0.0762 (2)	0.0795 (5)	0.3109 (3)
C(6)	0.1655 (2)	0.2727 (5)	0.4450 (4)
O(6)	0.2008 (2)	0.2915 (5)	0.4292 (4)
C(7)	0.0994 (2)	−0.0462 (5)	0.5067 (4)
O(7)	0.0709 (2)	−0.1074 (4)	0.4657 (3)
C(8)	0.1934 (2)	−0.0036 (6)	0.5144 (4)
O(8)	0.2184 (2)	−0.0338 (6)	0.4760 (4)
C(9)	0.1665 (2)	−0.0512 (5)	0.6824 (4)
O(9)	0.1757 (2)	−0.1091 (5)	0.7445 (4)
C(10)	0.1950 (2)	0.1728 (5)	0.6410 (4)
O(10)	0.2236 (1)	0.2390 (4)	0.6770 (4)
O(11)	0.1221 (1)	0.3291 (3)	0.5972 (2)
Si	0.12773 (5)	0.46953 (13)	0.62518 (11)
C(11)	0.1755 (3)	0.5302 (6)	0.5796 (7)
C(12)	0.1877 (4)	0.6577 (8)	0.5921 (11)
C(13)	0.0699 (3)	0.5513 (6)	0.5741 (6)
C(14)	0.0629 (3)	0.6626 (7)	0.6180 (6)
C(15)	0.1430 (2)	0.4823 (6)	0.7517 (5)
C(16)	0.1922 (3)	0.4386 (9)	0.8071 (5)
H(16)	0.060 (1)	0.186 (5)	0.505 (1)

---

(19) Sheldrick, G. M. SHELX76; University of Cambridge: Cambridge, England, 1976.

(20) *International Tables for X-ray Crystallography*; Kynoch: Birmingham, England, 1972; Vol. 4, pp 99–149.

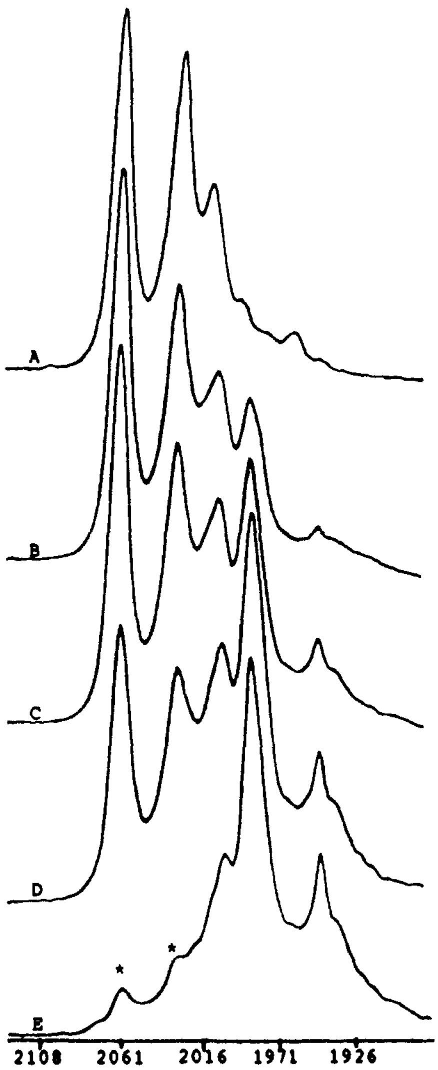

Figure 1. Time-dependent IR spectra resulting from the addition of Ph_3SiONa to $Ru_3(CO)_{12}$ (in THF): (A) $Ru_3(CO)_{12}$; (E) $[Ru_6(CO)_{18}]^{2-}$ and $[Ru_4(CO)_{13}]^{2-}$. The other spectra indicate mixtures of these species. (Asterisks represent residual $Ru_3(CO)_{12}$.)

positional parameters, including those of the H (hydride) atom [H(18)], are listed in Table III.

Scheme I

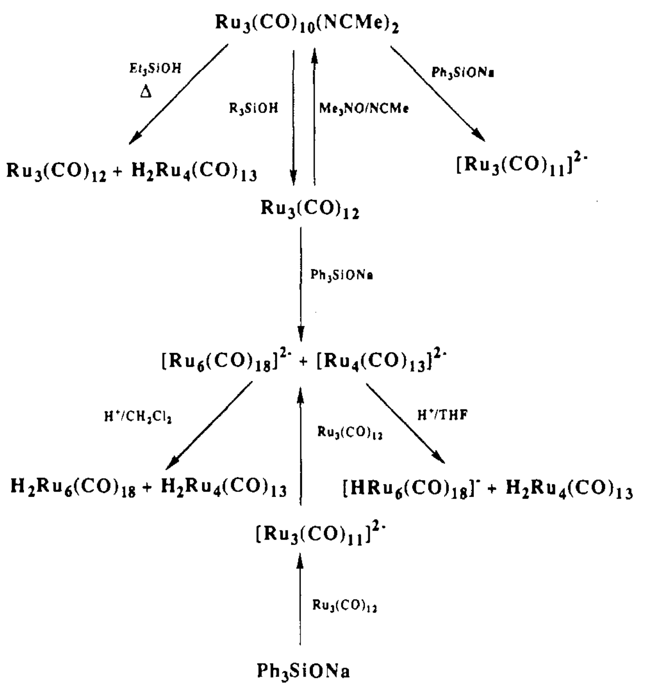

Results and Discussion

$Ru_3(CO)_{12-x}L_x$ (L = CO, NCMe; x = 1, 2) was allowed to react with Si and Al complexes under a variety of conditions. Transition-metal carbonyl clusters containing Al are largely unknown, but we report findings regarding the interaction of AlH_3 and $Et_3N{\cdot}AlH_3$ with $Ru_3(CO)_{12-x}L_x$.

Interaction of $Ru_3(CO)_{10}L_2$ (L = CO, NCMe) with R_3SiOH (R = Et, Ph) and Ph_3SiONa. $Ru_3(CO)_{10}(NCMe)_2$ was allowed to react with R_3SiOH (R = Et, Ph) at temperatures in the range 25–70 °C with NCMe, CH_2Cl_2, or Et_3SiOH as solvents. In all cases most of the ruthenium (ca. 80%) was recovered as $Ru_3(CO)_{12}$; however, the reaction carried out at 55 °C also yielded $H_2Ru_4(CO)_{13}$, with both compounds identified by IR spectroscopy. The interaction of $Ru_3(CO)_{10}(NCMe)_2$ with a 3-fold excess of Ph_3SiOH, dissolved in THF, yielded $[Ru_3(CO)_{11}]^{2-}$ as the main species in solution; however, when the silanolate derivative was added dropwise to a solution of $Ru_3(CO)_{12}$, formation of $[Ru_6(CO)_{18}]^{2-}$ (2003 m, 1988 s, 1931 w sh cm^{-1}) and $[Ru_4(CO)_{13}]^{2-}$ (1946 m cm^{-1}) was observed (Figure 1). Protonation of the anionic species in CH_2Cl_2 yielded $H_2Ru_6(CO)_{18}$ and $H_2Ru_4(CO)_{13}$, identified by their IR spectra (Figure 2A,B) and by the unit cell parameters obtained by single-crystal X-ray diffraction. These parameters are identical, within experimental error, with those reported.[21,22]

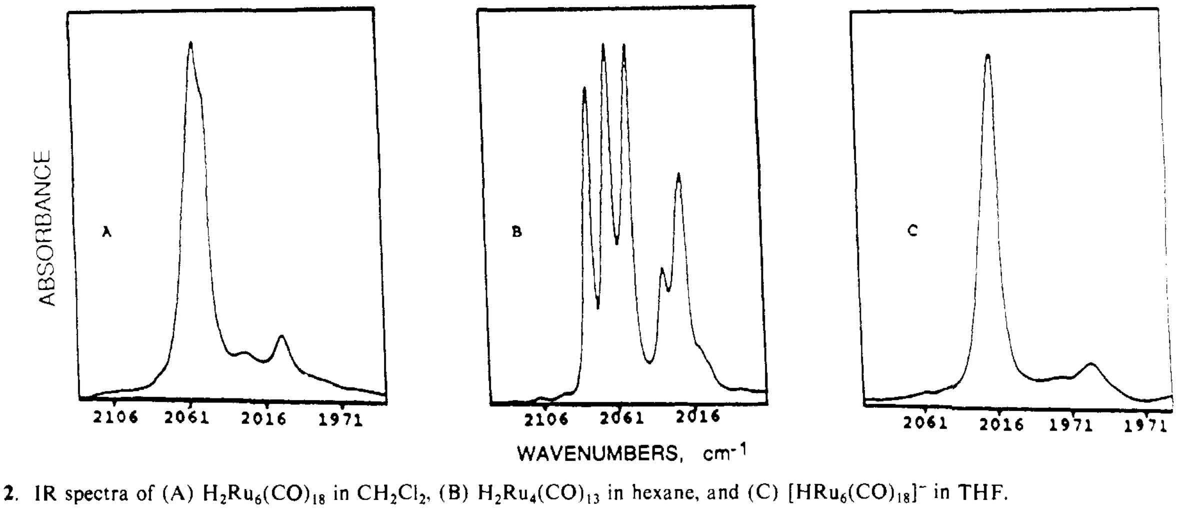

Figure 2. IR spectra of (A) $H_2Ru_6(CO)_{18}$ in CH_2Cl_2, (B) $H_2Ru_4(CO)_{13}$ in hexane, and (C) $[HRu_6(CO)_{18}]^-$ in THF.

Bhattacharyya et al.[23] have demonstrated that reduction of $Ru_3(CO)_{12}$ is effectively performed by alkali metal–benzophenone, with $[Ru_3(CO)_{11}]^{2-}$ being an intermediate in the formation of $[Ru_6(CO)_{18}]^{2-}$ and $[Ru_4(CO)_{13}]^{2-}$. The interaction of $Ru_3(CO)_{10}L_2$ with silanols and silanolate derivatives suggests that a similar reaction pathway occurs. Thus, slow addition of $Ru_3(CO)_{12}$ to a THF solution of Ph_3SiONa gave $[Ru_3(CO)_{11}]^{2-}$ as the predominant species in solution. Formation of $[Ru_6(CO)_{18}]^{2-}$ and $[Ru_4(CO)_{13}]^{2-}$ was observed upon further addition of $Ru_3(CO)_{12}$. Protonation of these anionic species, in THF, with H_2SO_4 was followed by extraction with hexane. Thin-layer chromatography of the extract yielded $H_2Ru_4(CO)_{13}$ (Figure 2B). The residue was extracted with diethyl ether and identified as $[HRu_6(CO)_{18}]^-$ (Figure 2C).[24]

These results show that interaction of $Ru_3(CO)_{12-x}L_x$ with R_3SiOH, and especially with Ph_3SiONa, occurs with reduction of the metal cluster. The product distribution is summarized in Scheme I. The extensive reduction of this trinuclear species by the silanolate group (Si–O$^-$) under mild conditions shows that the product distribution depends on the relative concentrations of the trinuclear cluster and the reducing agent, consistent with the work reported by Bhattacharyya et al.[23]

These observations are relevant to surface organometallic chemistry. Thus, reaction of $Ru_3(CO)_{12}$ with the reducing sites on the surface of an appropriate inorganic oxide support such as MgO would be expected to yield $[Ru_3(CO)_{11}]^{2-}$ (or $[HRu_3(CO)_{11}]^-$) as the principal ruthenium species, and further reaction in the presence of $Ru_3(CO)_{12}$ would be expected to lead to a mixture of anionic compounds similar to that described in Scheme I. Formation of either dianionic species (e.g., $[Ru_3(CO)_{11}]^{2-}$) or the corresponding hydride derivatives (e.g., $HRu_3(CO)_{11}]^-$) will depend on the nature of the reducing surface sites and be influenced by the degree of dehydroxylation of the support. This reactivity pattern is consistent with the mixture of ruthenium complexes $[Ru_3(CO)_{11}]^{2-}$, $[Ru_6(CO)_{18}]^{2-}$, and $[HRu_4(CO)_{13}]^-$ reported to be present on the surface of the basic MgO support upon chemisorption of $Ru_3(CO)_{12}$.[25]

Interaction of $Ru_3(CO)_{11}L$ (L = CO, NCMe) with AlH_3 and $Et_3N{\cdot}AlH_3$. Slow addition of AlH_3 to a solution of $Ru_3(CO)_{12}$ at −20 or −50 °C resulted in formation of $[HRu_3(CO)_{11}]^-$; further addition led to precipitation of a brown solid, leaving $[Ru_3(CO)_{11}]^{2-}$ as the major species remaining in solution. Protonation with HBF_4 followed by workup of the solution gave $H_2Ru_4(CO)_{13}$ and $H_4Ru_4(CO)_{12}$, consistent with the reduction of $Ru_3(CO)_{12}$ with bases or sodium amalgam.[26] Similar results were obtained when $Ru_3(CO)_{12}$ was treated with superhydride ($LiEt_3BH$) at −20 °C followed by addition of AlH_3 at the same temperature. Characterization of the precipitate was precluded by its poor solubility in hexane, dichloromethane, acetone, THF, and acetonitrile.

Interaction of $Et_3N{\cdot}AlH_3$ with $Ru_3(CO)_{12}$ in THF at room temperature, after stirring for ca. 12 h, did not give a significant conversion, with the trinuclear starting material still being the major ruthenium species in solution. After 4 days of stirring in the presence of $Et_3N{\cdot}AlH_3$, a dark brown precipitate, insoluble in dichloromethane, acetone, and ethyl acetate, was observed. Reaction of the Al derivative with $Ru_3(CO)_{11}(NCMe)$ resulted in rapid formation of $[Ru_3(CO)_{11}]^{2-}$; further addition of the Al reagent revealed formation of an unidentified brown solid.

Interaction of Et_3SiOH with $Ru_3(CO)_{12}$ in the Presence of $Cp_2Fe_2(CO)_4$. Investigations of the reactions of metal carbonyl compounds on metal oxide supports have shown that treatment of the supported species under appropriate reaction conditions allows stepwise increases in the nuclearity to yield well-defined molecular clusters on the surface.[27-29] The results of these investigations demonstrate that trinuclear species are intermediates formed on supports during cluster growth. Some attention has been devoted to the chemistry of $Ru_3(CO)_{12}$ on silica and to the catalytic activity of surface-bound species for the hydrogenation and isomerization of alkenes and the reduction of CO to give hydrocarbons.[30] Determination of the nature of these surface-bound species demands a range of physical techniques. EXAFS spectroscopy is particularly useful for the identification of the supported compounds and determination of bond distances, and it has been applied to alumina- and silica-supported metal clusters.[31-34] However, even with this method it has proved difficult in some instances to differentiate between feasible structural configurations having metal atoms with the same coordination number.[32] A valuable complementary approach involves the preparation and structural characterization of molecular models that incorporate groups similar to those present on the support surface (e.g., silanol groups).

Our efforts in the design of a synthetic route leading to the incorporation of the silanol ligand within the ruthenium framework were initially frustrated by the predominant reductive character of the silanol moiety. Consequently, as an alternative, a catalytic pathway was sought for insertion of ligands within the coordination sphere of the metal.[35] Our interest in this approach was stimulated particularly by a recent report describing the catalytic incorporation of alcohols within the $Ru_3(CO)_{12}$ framework.[36] Thus, $Ru_3(CO)_{12}$ was allowed to reflux in cyclohexane in the presence of Et_3SiOH, and then $Cp_2Fe_2(CO)_4$ was added in catalytic amounts. After reaction, the solvent was evaporated, the product was extracted with pentane, and the extract was concentrated under vacuum. Thin-layer chromatography, with hexane as the eluent, showed a top orange band, 7% yield, characterized as $(\mu\text{-H})Ru_3(CO)_{10}(\mu\text{-OSiEt}_3)$ (**1**) by IR (hexane: 2105 w, 2068 vs, 2057 s, 2022 vs, 2008 s, 2000 m sh, 1995 m cm^{-1}) and ^1H NMR spectroscopy ($CDCl_3$: 0.97 t, 0.5 q, −12.08 s ppm; integration ratio 9:6:1) and mass spectrometry (m/e 715, ^{101}Ru, ^{28}Si, a fragmentation pattern corresponding to sequential loss of 10 CO's).

When a 5-fold larger amount of $Cp_2Fe_2(CO)_4$ was used ($Ru_3(CO)_{12}$:$Cp_2Fe_2(CO)_4$ molar ratio 2:1), virtually the same yield was obtained. Under the same reaction conditions, the triphenylsilanol derivative could not be prepared. An increased reaction temperature resulting from use of a higher boiling point solvent did not lead to the desired product. The catalytic action of the iron dimer has been explained in terms of thermally generated radicals.[36]

Structural characterizations of siloxyl-bridged diruthenium complexes have been reported recently, but no metal–metal bond is present in these complexes.[37] Complex **1** represents, on the other hand, a suitable molecular analogue of the grafted cluster $HRu_3(CO)_{10}(OSi{<})$ (**2**) obtained from the uncatalyzed reaction of $Ru_3(CO)_{12}$ with a silanol group of the silica surface.[38] The

---

(21) Churchill, M. R.; Wormald, J. *J. Am. Chem. Soc.* **1971**, *93*, 5670–677.
(22) Yawney, D. B. W.; Doedens, R. J. *Inorg. Chem.* **1972**, *11*, 838–844.
(23) Bhattacharyya, A. A.; Nagel, C. C.; Shore, S. G. *Organometallics* **1983**, *2*, 1187–1193.
(24) Eady, C. R.; Jackson, P. F.; Johnson, B. F. G.; Lewis, J.; Malatesta, M. C.; McPartlin, M.; Nelson, W. J. H. *J. Chem. Soc., Dalton Trans.* **1980**, 383–392.
(25) Krause, T. R. Ph.D. Thesis, University of Delaware, 1987.
(26) Johnson, B. F. G.; Lewis, J.; Kilty, P. A. *J. Chem. Soc. A* **1968**, 2859–2864.
(27) Fung, A. S.; Tooley, P. A.; Kelley, M. J.; Gates, B. C. *J. Chem. Soc., Chem. Commun.* **1988**, 371–372.
(28) Lamb, H. H.; Gates, B. C. *J. Am. Chem. Soc.* **1986**, *108*, 81–89.
(29) Lamb, H. H.; Fung, A. S.; Tooley, A. P.; Puga, J.; Kelley, M. J.; Gates, B. C. *J. Am. Chem. Soc.* **1989**, *111*, 8367–8373.
(30) Gates, B. C.; Guczi, L.; Knözinger, H., Eds.; *Metal Clusters in Catalysis*; Elsevier: Amsterdam, 1986; p 462.
(31) Duivenvoorden, F. B.; Koningsberger, D. C.; Uh, Y. S.; Gates, B. C. *J. Am. Chem. Soc.* **1986**, *108*, 6254–6262.
(32) Binsted, N.; Evans, J.; Greaves, G. N.; Price, R. S. *Organometallics* **1989**, *8*, 613–620.
(33) Cook, S. L.; Evans, J.; Greaves, G. N. *J. Chem. Soc., Chem. Commun.* **1983**, 1287–1289.
(34) Alexiev, V. D.; Binsted, N.; Evans, J.; Greaves, G. N.; Price, R. J. *J. Chem. Soc., Chem. Commun.* **1987**, 395–397.
(35) Wang, S.-J.; Angelici, R. J. *Inorg. Chem.* **1988**, *27*, 3233–3235 and references therein.
(36) Aime, S.; Botta, M.; Gobetto, R.; Osella, D.; Padovan, F. J. *J. Chem. Soc., Dalton Trans.* **1987**, 253–254.
(37) Bruce, G. C.; Stobart, S. R.; *Inorg. Chem.* **1988**, *27*, 3880–3885.

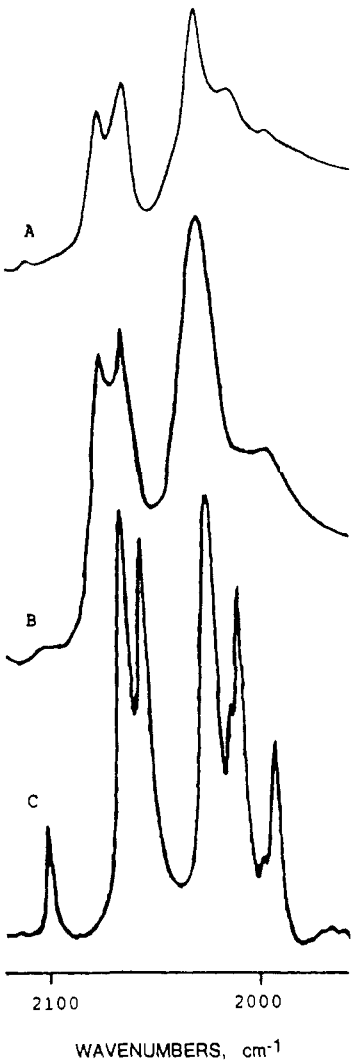

Figure 3. IR spectra of (A) (μ-H)Os$_3$(CO)$_{10}$(μ-OSi$<$) in the solid state, (B) (μ-H)Ru$_3$(CO)$_{10}$)(μ-OSi$<$) in the solid state,[26] and (C) (μ-H)Ru$_3$(CO)$_{10}$(μ-OSiEt$_3$) in hexane.

synthesis and full characterization of **1** substantiates the feasibility of the configuration assigned to **2**. Inspection of the IR data for **1** and **2** (Figure 3) confirms the analogy between the two structures and the suitability of the model. To determine unambiguously the coordination mode of the silanol group and the position of the hydride ligand, further characterization of (μ-H)Ru$_3$(CO)$_{10}$(μ-OSiEt$_3$) was carried out by single-crystal X-ray analysis of a sample obtained by slow evaporation from a dichloromethane–hexane mixture.

Description of the Structure. The molecular structure of (μ-H)Ru$_3$(CO)$_{10}$(μ-OSiEt$_3$) is shown with the atomic labeling in Figure 4. Relevant bond distances and angles are listed in Table I. Compound **1** is isostructural, and its crystals are isomorphous, with the analogous Os cluster (μ-H)Os$_3$(CO)$_{10}$(μ-OSiEt$_3$).[10]

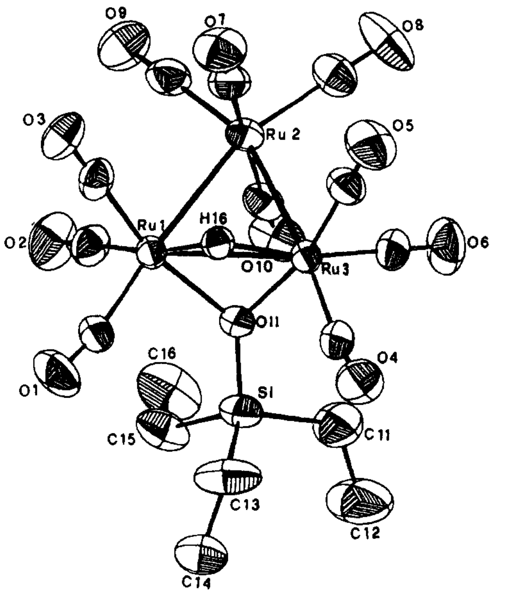

Figure 4. ORTEP diagram of **1** showing 50% thermal ellipsoids. C atoms of the CO groups bear the same numbering as the corresponding O atoms. H atoms of the C$_2$H$_5$ groups are omitted for clarity. The H (hydride) position is shown.

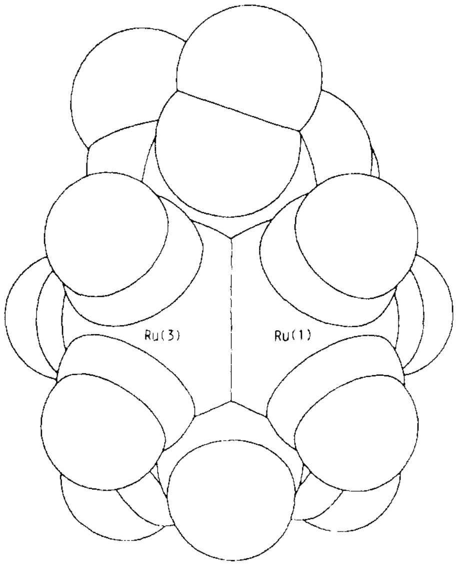

Figure 5. Space-filling view of the plane defined by CO's 1, 3, 4, and 5 showing the niche in which the H (hydride) atom is accommodated.

The metal atom framework consists of a nearly isosceles triangle having two "long" [mean 2.794 (1) Å] and one "short" [Ru(1)–Ru(3) = 2.753 (1) Å] edges, similar to that found for the Os analogue.[10] The short bond in the triruthenium cluster is bridged by the μ-OSiEt$_3$ ligand and by the H (hydride) atom. An important result of this structure determination is the location of this latter atom bridging the Ru(1)–Ru(3) bond [Ru–H = 1.75 (1), 1.74 (1) Å]. Although the direct location of H atoms by X-ray diffraction in metal clusters of this complexity is problematical, our observation is supported by the indirect information contained in the space-filling diagram depicted in Figure 5. This clearly shows how the CO ligands around this edge are pushed away from its center, leaving a large niche for accommodation of the H atom. Further, the Ru–H distances obtained agree with values derived from neutron diffraction studies of species that have similar μ-H bridges.[39,40] Thus, **1** is electron precise and isoelectronic with Ru$_3$(CO)$_{12}$. The lengthening effect, which usually accompanies formation of a three-center two-electron bond upon H-bridging, is here counterbalanced by an effect in the opposite direction due to the μ-OSiEt$_3$ ligand.

The Ru(2)–C distances are longer in mean value [1.929 (6) Å] than the Ru(1)–C and Ru(3)–C distances [mean 1.904 (6) Å]; the bonds belonging to this latter set are spread over a large range [Ru(1), 1.870 (6)–1.950 (6); Ru(3), 1.859 (6)–1.965 (6) Å]. The longest interactions are with the CO groups directed along the unbridged Ru–Ru bonds, and the shortest ones are involved with the two ligands transoid to the two Ru–O bonds.

---

(38) Theolier, A.; Choplin, A.; D'Ornelas, L.; Basset, J. M.; Zanderighi, G.; Ugo, R.; Psaro, R.; Sourisseau, C. *Polyhedron* **1983**, *2*, 119–121.

(39) Zhu, N. J.; Lecomte, C.; Coppens, P.; Keister, J. B. *Acta Crystallogr.* **1982**, *B38*, 1286–2287.

(40) Catti, M.; Gervasio, G.; Mason, S. A. *J. Chem. Soc., Dalton Trans.* **1977**, 2260–2264.

The two Ru–O distances are nearly identical [2.106 (3), 2.107 (3) Å] and only slightly shorter than the Os–O distances in the Os analogue [2.118 (6) Å]. The Ru–O distances compare well with Ru–O distances observed in some dinuclear Ru species having similar groups.[37] Altogether, the bond length distribution in **1** conforms well to the molecular quasi *m* symmetry (the pseudomirror plane passing through Ru(2) and the midpoint of the Ru(1)–Ru(3) bond). Such molecular symmetry is in fact broken only by the Si–Et group orientations.

Implications for Surface Organometallic Chemistry. Interaction of the silanol and silanolate derivatives with the triruthenium clusters in the absence of catalytic amounts of $Cp_2Fe_2(CO)_4$ resembles the reactivity pattern encountered upon chemisorption of $Ru_3(CO)_{12}$ on the basic MgO support, in which exlusively reduction products are observed. In contrast, oxidative addition of a surface silanol group to the metal–metal bond of $Ru_3(CO)_{12}$ occurs upon chemisorption of the trinuclear cluster on silica. Although the different reactivity patterns are probably a consequence of the intrinsic properties of the SiO_2 surface, the oxidative addition pathway may require activation of a carbonyl ligand in a manner similar to that proposed for the catalytic action of the iron dimer.

The synthesis of **1** was made possible by the presence of catalytic amounts of $Cp_2Fe_2(CO)_4$. This result suggests that a similar approach may be a viable alternative for incorporating species within the coordination sphere of a metal cluster, which tends to yield reduction products exclusively.

Acknowledgment. We are grateful to Dr. A. L. Rheingold of the University of Delaware for the determination of the unit cell parameters for $H_2Ru_4(CO)_{13}$ and $H_2Ru_6(CO)_{18}$. This work was supported by the National Science Foundation (Grants CBT-8605699, CHE 86-02941, and CHE 87-01413).

Supplementary Material Available: Tables of crystal data, anisotropic thermal parameters, fractional atomic coordinates and thermal parameters, fractional atomic coordinates and thermal parameters for the hydrogen atoms, and complete bond distances and angles (27 pages); F_o/F_c tables (20 pages). Ordering information is given on any current masthead page.

Contribution from the Department of Chemistry,
Washington State University, Pullman, Washington 99164-4630

Solvent, Anion, and Temperature Dependences of the Ruthenocene(II)/Bromoruthenocene(IV) and Ruthenocene(II)/Iodoruthenocene(IV) Electron Exchange

Karl Kirchner, Harold W. Dodgen, Scot Wherland, and John P. Hunt*

Received May 1, 1989

The rates of the electron exchange between $Ru(cp)_2$ and $Ru(cp)_2Br^+$ (cp represents the cyclopentadienide anion) as the PF_6^-, ClO_4^-, and BF_4^- salts and between $Ru(cp)_2$ and $Ru(cp)_2I^+$ as the $CF_3SO_3^-$ and PF_6^- salts have been measured by ^1H NMR line broadening as a function of temperature and solvent. The observed second-order rate constants at 20 °C and the activation parameters obtained for the $Ru(cp)_2/Ru(cp)_2Br^+$ system as the PF_6^- salt are as follows ($10^{-3}k$ in $M^{-1}\ s^{-1}$, ΔH^* in kcal mol^{-1}, ΔS^* in cal $mol^{-1}\ K^{-1}$): nitrobenzene-d_5, 2.9 ± 0.2, 8.1 ± 0.1, −14.8 ± 0.2; nitromethane-d_3, 2.5 ± 0.1, 8.5 ± 0.1, −14.1 ± 0.5; acetonitrile–d_3, 1.6 ± 0.08, 8.2 ± 0.1, −15.7 ± 0.3; benzonitrile, 1.6 ± 0.08, 8.6 ± 0.3, −14.5 ± 1.1. For the $Ru(cp)_2/Ru(cp)_2I^+$ system as the $CF_3SO_3^-$ salt, the second-order rate constants at 20 °C and the activation parameters obtained are as follows ($10^{-5}k$ in $M^{-1}\ s^{-1}$, ΔH^* in kcal mol^{-1}, ΔS^* in cal $mol^{-1}\ K^{-1}$): nitrobenzene-d_5, 2.6 ± 0.1, 6.6 ± 0.1, −11.3 ± 0.3; nitromethane-d_3, 19.2 ± 1.0, 8.5 ± 0.3, −0.5 ± 0.7; acetonitrile-d_3, 7.4 ± 0.4, 6.7 ± 0.2, −8.7 ± 0.8. Only a slight dependence on extra added salt is found for the above solvents. In the low dielectric constant solvents, chloroform-d_1, bromobenzene-d_5, and methylene-d_2 chloride, ion association occurs and thus the observed rate constants and activation parameters are composite quantities from free-ion and ion-paired pathways. For chloroform-d_1, the rate constants for two pathways are resolved. The calculations indicate that the electron-transfer reaction does not occur appreciably via the ion-paired pathway. There is no significant dependence of rate on the identity of the counterion. Decamethylruthenocene(II) does not exchange with bromo- or iododecamethylruthenocene(IV) even at 110 °C in nitrobenzene-d_5.

Introduction

The study of one-electron-transfer reactions between substitution-inert monometallic transition-metal complexes in nonaqueous solution has become an appealing area of research in recent years. Consequently, considerable progress has been made in both experimental and theoretical respects.[1-3] However, reports on multielectron-transfer reactions between monometallic transition-metal complexes are sparse.[4] A prototypical example of a simple two-electron, apparently inner-sphere, exchange reaction was introduced by Taube et al., namely the halogen-mediated electron transfer between metallocenes of ruthenium and osmium in the oxidation states 4+ and 2+.[5] The reactants are stable in both oxidation states in solution over a large range of temperatures and pressures. A comparison of solvent electrolyte effects between inner-sphere and outer-sphere electron-exchange reactions might be of interest.

In these two-electron-transfer reactions, structural changes that accompany charge transfer and the activation process will be in contrast with those of simple outer-sphere self-exchange reactions. Variation of solvent, temperature, electrolyte, and anion may give a deeper insight into the detailed mechanism of this reaction type. Other important questions concerning two-electron transfers are how the halogen exerts control on the reaction, whether a concerted two-electron process occurs or whether two one-electron steps are involved, and if the latter occurs, whether Ru(III) intermediates can be detected.

In this paper we report an investigation of the kinetics for various temperatures, solvents, and anions for the ruthenocene/bromoruthenocene and ruthenocene/iodoruthenocene electron-exchange reactions.

Experimental Section

Materials. Ruthenocene was obtained from Strem Chemicals, Inc., and was purified by one vacuum sublimation. $[Ru(cp)_2Br]X$ ($X = PF_6^-$, BF_4^-, ClO_4^-) and $[Ru(bp)_2I]X$ ($X = CF_3SO_3^-$, PF_6^-) were synthesized according to refs 6 and 7. $[Ru(cp)_2Br]X$ was recrystallized twice from

---

(1) Cannon, R. D. *Electron Transfer Reactions*; Butterworth: London, 1980.

(2) Sutin, N. *Acc. Chem. Res.* **1982**, *15*, 275.

(3) Sutin, N. *Prog. Inorg. Chem.* **1983**, *30*, 441.

(4) Finke, R. G.; Voegeli, R. H.; Laganis, E. D.; Boekelheide, V. *Organometallics* **1983**, *2*, 347.

(5) Smith, T. P.; Iverson, D. J.; Droege, M. W.; Kwan, K. S.; Taube, H. *Inorg. Chem.* **1987**, *26*, 2882.

(6) Smith, T. P.; Kwan, K. S.; Taube, H.; Bino, A.; Cohen, S. *Inorg. Chem.* **1984**, *23*, 1943.

(7) Sohn, Y. S.; Schlueter, A. W.; Hendrickson, D. N.; Gray, H. B. *Inorg. Chem.* **1974**, *13*, 301.